International Journal of Pharmaceutics 661 (2024) 124418

Contents lists available at ScienceDirect

International Journal of Pharmaceutics

journal homepage: www.elsevier.com/locate/ijpharm

Hydrophobic deep eutectic solvent (HDES) as oil phase in lipid-based drug formulations

Shaida Panbachi [a,b,c], Josef Beranek [a], Martin Kuentz [c,*]

[a] Zentiva, k.s., U Kabelovny 130 102 00, Praha 10, Czech Republic
[b] University of Basel, Department of Pharmaceutical Sciences, Klingelbergstrasse 50 4056, Basel, Switzerland
[c] University of Applied Sciences and Arts Northwest. Switzerland, School of Life Sciences, Institute of Pharma Technology, Hofackerstr. 30 CH- 4132, Muttenz, Switzerland

ARTICLE INFO

Keywords:
Deep eutectic solvent(s)
Eutectic(s)
Poorly soluble drug(s)
Lipid-based formulation(s)
Novel pharmaceutic(s)
Advanced formulation(s)

ABSTRACT

There is increasing pharmaceutical interest in deep eutectic solvents not only as a green alternative to organic solvents in drug manufacturing, but also as liquid formulation for drug delivery. The present work introduces a hydrophobic deep eutectic solvent (HDES) to the field of lipid-based formulations (LBF). Phase behavior of a mixture with 2:1 M ratio of decanoic- to dodecanoic acid was studied experimentally and described by thermodynamic modelling. Venetoclax was selected as a hydrophobic model drug and studied by atomistic molecular dynamics simulations of the mixtures. As a result, valuable molecular insights were gained into the interaction networks between the different components. Moreover, experimentally the HDES showed greatly enhanced drug solubilization compared to conventional glyceride-based vehicles, but aqueous dispersion behavior was limited. Hence surfactants were studied for their ability to improve aqueous dispersion and addition of Tween 80 resulted in lowest droplet sizes and high in vitro drug release. In conclusion, the combination of HDES with surfactant(s) provides a novel LBF with high pharmaceutical potential. However, the components must be finely balanced to keep the integrity of the solubilizing HDES, while enabling sufficient dispersion and drug release.

1. Introduction

Deep eutectic solvents (DES) have been reported as an attractive solubilization technology with potentially a several thousand-fold increase in solubility relative to water (Faggian et al., 2016; Fourmentin et al., 2021; Jeliński et al., 2019; Li & Lee, 2016; Sut et al., 2017). Several studies have also shown that this holds true when dissolving pharmaceutically active ingredients (APIs) that are otherwise poorly soluble (Faggian et al., 2016; Fourmentin et al., 2021; Huber et al., 2022; Li & Lee, 2016; Morrison et al., 2009; Palmelund et al., 2019). Notable examples include aprepitant and indomethacin, where solubility in the respective DES yielded 6.78 ± 0.03 mg/g (1057-fold higher than the aqueous solubility) for the former and 175.6 ± 3.428 mg/mL (≈ 159′000- fold higher than the aqueous solubility) for the latter API (Palmelund, Eriksen, et al., 2021; Panbachi et al., 2023). DES are generally considered as a worthwhile alternative to organic solvents and ionic liquids due to potentially better oral tolerability (Benvenutti et al., 2019; Dai et al., 2013; Fourmentin et al., 2021; Hansen et al., 2021; Ramón & Guillena, 2019). Traditionally, DES have mainly been studied and utilized in the field of green chemistry and chemical engineering, mostly by relying on the strong solubilization effects of the liquids applied (Fourmentin et al., 2021; Hansen et al., 2021; Martins et al., 2019; Morrison et al., 2009; Ramón & Guillena, 2019). However, these mixtures also present great underexplored potential in the field of pharmaceutics where such mixtures could either hold for an intermediate bulk solution or even the final drug product (Abranches & Coutinho, 2023; Oyoun et al., 2023; Palmelund, Eriksen, et al., 2021; Palmelund et al., 2019; Panbachi et al., 2023).

A deep eutectic solvent (DES) is described as a mixture of two or more hydrogen bond acceptors (HBAs) and donors (HBDs), interacting at a specific molar ratio, resulting in a eutectic point that is lower than that of the hypothetical eutectic point at ideal conditions (Abranches & Coutinho, 2023; Fourmentin et al., 2021; Hansen et al., 2021; Martins et al., 2019). This is the distinct characteristic of DES (Martins et al., 2019). Furthermore, these liquids have been described as thermodynamically stable in their liquid state and can be liquid at room- and/or operating temperatures depending on their eutectic point (Abdelquader et al., 2023; Ghaedi et al., 2018). These beneficial properties make DES a

* Corresponding author.
E-mail address: martin.kuentz@fhnw.ch (M. Kuentz).

https://doi.org/10.1016/j.ijpharm.2024.124418
Received 25 April 2024; Received in revised form 28 June 2024; Accepted 1 July 2024
Available online 2 July 2024

viable option in the development of a solubility-improving formulation for poorly water-soluble APIs (Abdelquader et al., 2023; Palmelund, Eriksen, et al., 2021; Panbachi et al., 2023).

As mentioned above, the clear deviation in thermodynamic behavior of DES from the ideal melting point depression, distinguishes it from other eutectic solutions (Martins et al., 2019). This can be deemed a 'strict' definition of a DES, because previous literature often used the term broadly from a practical application point of view without providing phase diagrams. Therefore, several DES experts recently encouraged researchers to supply newly described DES with phase diagrams to better distinguish eutectic mixtures from true DES (Abranches & Coutinho, 2023; Martins et al., 2019; Palmelund, Rantanen, et al., 2021). Accordingly, the current work provides such phase diagrams using the Schröder van Laar (SvL) equation, thereby describing a solid–liquid line for 'ideal' mixture conditions (i.e., using an activity coefficient of 1), which is compared to an experimental phase diagram (Palmelund et al., 2020; Wolbert et al., 2019). Moreover, universal quasichemical functional group activity coefficients (UNIFAC) were considered as a predictive thermodynamic model to compare with experimental data and to identify possible model improvements compared to the ideal SvL equation. This approach has been pioneered in the field of therapeutic DESs (THEDESs) by Wolbert et al., 2019. As a result, the UNIFAC model proved to be adequate to describe the selected model systems. More work should be done based on this thermodynamic approach to study not only THEDESs, where the drug is a constituting deep eutectic component, but also DES as a solvent mixture for drugs.

DES are divided into 5 categories of mixtures (I-V) depending on the chemistry of the components employed (Abranches et al., 2019; Fourmentin et al., 2021). Type III DESs are made of organic HBD and HBAs, which have been described as the most suitable candidates for pharmaceutical development due to their comparatively better oral tolerability (Abdelquader et al., 2023; Abranches & Coutinho, 2023; Fourmentin et al., 2021; Oyoun et al., 2023; Palmelund et al., 2019). Within this category, further subcategories can be described based on the properties of the constituent components, which ultimately determine the physicochemical properties of the final DES formulation. For example, natural deep eutectics, a known subcategory of class III deep eutectics, are referred to as "natural" due to the use of components with natural origins; these include primary metabolites such as organic acids, amino acids, sugars, polyols, and choline derivatives, which show low toxicity (Fourmentin et al., 2021). These "natural" DES or NADES have been deemed viable candidates for drug product development and environmental applications (Dai et al., 2013; Faggian et al., 2016; Fourmentin et al., 2021; Huber et al., 2022; Jeliński et al., 2019; Liu et al., 2018; Sut et al., 2017).

Another example of components that govern final DES formulation properties are hydrophobic deep eutectic solvents (HDESs). These are another subcategory of class III DES comprised of hydrophobic components (Florindo et al., 2018; Fourmentin et al., 2021; Ramón & Guillena, 2019; Van Osch et al., 2020; Zainal-Abidin et al., 2021). They have been described in the literature and studied for their extraction capabilities in chemical sustainability and engineering (Florindo et al., 2018; Van Osch et al., 2020; Zainal-Abidin et al., 2021). However, to our knowledge, HDES have not been studied for pharmaceutical applications (Van Osch et al., 2020). Using HDES either directly or with further added excipient (s), could pave the way for novel pharmaceutical applications.

In this study, an HDES is investigated as an alternative to traditionally used oils in lipid-based formulations (LBFs) to enable a viable formulation of venetoclax. The latter drug is known to be a BCS (biopharmaceutical classification system) class IV API (Emami Riedmaier et al., 2018; Shah & Amidon, 2014) that does not meet the criteria of 'Lipinski's rule of 5' (DeGoey & Cox, 2021; Hartung et al., 2023) and the compound shows a high lipophilicity (logP $>$ 4) (Koehl et al., 2019, 2021). It is a hypothesis of the current work that HDES could be a useful formulation approach for overcoming the biopharmaceutical drug delivery issues of such APIs. The particular HDES used in this study is made of a 2:1 M ratio of decanoic acid (DeA) to dodecanoic acid (DoA), which has previously been described in two articles on extraction techniques and environmental chemistry (Dwamena, 2019; L. Wang & Meng, 2010). The present study targeted novel pharmaceutical applications by first studying the phase behavior, both experimentally and theoretically, using SvL and UNIFAC modelling. It also aimed to achieve a molecular understanding by using full atomistic molecular dynamics (MD) simulations of the pure DES as well as of the DES mixtures containing venetoclax. A further study aim was to explore the aqueous dispersion behavior of the selected HDES by considering surfactant addition (Tween 80) for development of an innovative lipid-based formulation (LBF).

2. Materials and methods

Venetoclax was purchased from Laurus Labs Ltd. (Telangana, India). The DES components decanoic acid (DeA) and dodecanoic acid (DoA), the surfactants Cremophor EL, DL-α-tocopherol methoxypolyethylene glycol succinate (TPGS) and Poloxamer 188, along with buffer components, HPLC-grade acetonitrile (≥99.9 %), ammonium phosphate monobasic and phosphoric acid solution for pH adjustments, were all purchased from Sigma-Aldrich (Sigma-Aldrich, Steinheim, Germany). Medium chain triglyceride Miglyol® 812 N was kindly provided as a free sample from IOI Oleochemicals (IOI Oleo GmbH, Hamburg, Germany). Gelucire 48/16, Labrasol ALF, Labrafac lipophile WL 1349, and Labrafil M2125 CS were also provided as free samples from Gattefossé (Saintpriest, France), and the Soluplus® was purchased from BASF (BASF SE, Ludwigshafen, Germany). Tween 80 (Ph.Eur. grade) was purchased from Carl Roth GmbH & Co. KG (Karlsruhe, Germany) and food-grade sesame oil was purchased from Momentum Foods Pty Ltd. (Melbourne, Australia).

2.1. Preparation and physical characterization of HDES

The hydrophobic deep eutectic solvent (HDES) consisted of decanoic acid (DeA) and dodecanoic acid (DoA) at the molar ratio of 2:1. The mixture was placed on a heating plate set to 70 °C, and stirred for 2 h (Dwamena, 2019). The maximum batch sizes prepared were 60 g and prepared HDESs were stored in an oven at a constant temperature of 25 °C.

The dynamic viscosity of the prepared liquid was measured in triplicate at ambient room temperature using the Turning Fork Vibro Viscometer SV-10A (A&D Company Ltd., Tokyo, Japan) at 30 Hz vibration. Prior to measurement, the instrument was adjusted using a one-point calibration method with water as the standard reference. Density was measured in triplicate at ambient temperature using oscillation that was induced electromagnetically in the glass U-tube of the DA-100 M densitometer (Mettler Toledo, Greifensee, Germany). The measurement was performed in triplicate on 1 mL samples injected into the tube.

Water content was measured in triplicate by a volumetric Karl-Fischer titration (KFT) instrument (Titrando 841 KFT, Metrohm Schweiz AG, Herisau, Switzerland). The titration factor was determined by the titration of 30 μL purified water using a 1 mL graduated calibrated microliter syringe with cemented needle (Hamilton Storage GmbH, Domat, Switzerland) and Titrant 5 as the titrant. The prepared HDES samples were diluted with methanol to give a solution with a concentration of 1 g/mL of water-containing-HDES in solvent. A 1 mL plastic syringe (Injekt®-F Luer Solo syringe, B. Braun Medical AG, Sempach, Switzerland) fitted with a needle (100 Sterican®, 20 G x 1 ½, B. Braun Medical AG, Sempach, Switzerland) was then used to inject 1 mL of the solution in the titration medium (Aqustar®, Merck KGaA, Taufkirchen, Germany). The water content and titration graph were then obtained by the Tiamo software version 2.4 (Metrohm, Herisau, Switzerland).

2.2. In-silico prediction of HDES phase diagram

The melting point of the individual molar ratios of the HDES was calculated using the Schröder van Laar equation (Prigogine & Defay, 1954; Umerska et al., 2020). This equation is derived from the Van't Hoff equation (Deiters, 2012) by assuming an ideal thermodynamic binary system where the activity coefficient (γ_i) is equivalent to one (Deiters, 2012; Prigogine & Defay, 1954; Wolbert et al., 2019). The following equation (1) describes the liquid–solid phase equilibrium, which corresponds to the Schröder van Laar equation in the event that the activity coefficient γ_i is unity (Chakraborty et al., 2021; Prigogine & Defay, 1954; Umerska et al., 2020; Wolbert et al., 2019):

$$\ln(\chi_i\ \gamma_i) = -\frac{\Delta H_i}{R}\left(\frac{1}{T} - \frac{1}{T_{m_i}}\right) \quad (1)$$

The equation includes temperature T, melting point T_{m_i} of a component i based on the molar fraction (χ_i), and the fusion enthalpy (ΔH_i) of component i (Prigogine & Defay, 1954). This equation is applied to both components in selected molar fractions from 0 to 1, increasing with consecutive 0.005 increments resulting in two different solid–liquid lines (SL-line) (Prigogine & Defay, 1954; Umerska et al., 2020; Wolbert et al., 2019). The trendlines of the two SL-lines are combined on a 'two-way' x-axis depicting the incremental increase in the molar fraction of one component from left to right, and the other component from right to left, where the intersection of the two lines provides the eutectic point on the phase diagram (Wolbert et al., 2019). When predicting the thermodynamic system's behavior in 'ideal conditions', the activity coefficient (γ_i) in equation (1) is unity (SvL), while activity coefficients were also calculated according to the UNIFAC approach as described below.

2.2.1. Prediction of activity coefficients using UNIFAC

The UNIFAC model is a universal quasichemical functional group contribution model to predict the activity coefficients of nonelectrolyte liquid mixtures (Fredenslund et al., 1975). The model assumes short-range order and long-range disorder and that the thermodynamic properties of a mixture are largely determined by the first neighbor's interactions (Abusleme & Vera, 1985; Fredenslund et al., 1975; Skjold-Jorgensen et al., 1979). UNIFAC is based on group contributions in that a molecule is split into different structural/functional groups where every group has specific group parameters and interaction parameters with other groups. Each molecule can be assembled based on these building blocks within the model to enable calculation of diverse chemicals. Since no experimental data is needed, UNIFAC is a fully predictive method to estimate activity coefficients (Abusleme & Vera, 1985; Fredenslund et al., 1975; Skjold-Jorgensen et al., 1979; Wolbert et al., 2019). Molecular Modeling Pro Flavor Plus (version 9.1.20) was used as an extension tool on the ChemElectrica gateway software (version 4.0.5) to calculate the respective UNIFAC activity coefficients. The values were estimated for standard conditions at 298.15 K, thereby avoiding the temperature dependence that was previously evaluated to have only minor effects (i.e., on the third decimal) on estimated activity coefficients.

2.3. Depiction of phase diagram using experimentally obtained melting points

The HDES experimental phase diagram was determined by depicting the mixture's solid–liquid line from melting points of different molar fractions of the two components (Wolbert et al., 2019). The melting point was measured using the differential scanning calorimetry (DSC) Pyris 1 (Perkin Elmer Inc., Norwalk, USA) connected to a cooling system (Perkin Elmer Inc., Norwalk, USA) programmed to perform a ramp cycle from −10 °C to + 50 °C, with a nitrogen purge of 50 mL/min, at a heating rate of 1 °C/min. The molar fractions of the physical mixtures studied increased incrementally from 0:1 to 1:0 of DeA:DoA. Two additional molar fractions corresponding to those derived from the predicted eutectic points (section 2.2), were also investigated.

To avoid spontaneous formation of the HDES during preparation, the physical mixtures were prepared using refrigerated components (−21 °C). The mixtures were briefly ground using a pestle and mortar in a cooled environment using cooling packs in a Styrofoam box, after which the samples were immediately refrigerated again (5 ± 3 °C). 5–8 mg of the prepared samples were transferred into standard aluminum pans (Perkin Elmer Inc., Norwalk, USA), and sealed with standard aluminum covers (Perkin Elmer Inc., Norwalk, USA). The DSC sample chamber was cooled to −10 °C prior to the measurement to ensure that the DSC sample chamber temperature would not result in spontaneous melting of the components. The thermograms obtained were analyzed using the Pyris software (version 11.1.0.0488). The endothermic peaks on the thermograms (determined in triplicate) were directed upwards and the onset point of the most prominent peak was selected as the melting point of the respective mixture to construct the solid–liquid line of the mixture (Umerska et al., 2020; Wolbert et al., 2019).

2.4. Molecular dynamics simulations of HDES

The molecular dynamics (MD) simulations were performed using the YASARA software version 20.12.24 (YASARA Biosciences GmbH, Vienna, Austria) (Krieger & Vriend, 2014). The simulations were based on pure HDES (DeA:DoA, 1:2) and HDES with 5 % w/w venetoclax (each with n = 4 simulation runs). To fit a cuboid simulation box with the dimensions of 65x65x65 Å, a number of 496 molecules of DeA and 248 molecules of DoA was selected to represent the pure HDES. The 5 % w/w venetoclax loaded system was analogous with eight molecules of API in the simulation box. An AMBER-type all atom force field (GAFF2) (Wang et al., 2004) was selected, for which atom charges were based on a semi-empirical quantum chemical estimation (AM1BCC) (Jakalian et al., 2002); long-range interactions were estimated using an 8 Å cut-off value for the mesh Ewald method as implemented in YASARA. To bring about initial random molecular orientations, an initial closed wall (i.e., NVT) cycle was run at 600 K for 5 ns, whereby the motion equations were integrated with 2x 1 fs steps. The main simulation cycle was then run using an NPT ensemble for a total time of 20 ns (2x 1 fs steps), using the set temperature of 298 K under periodic boundary conditions. The temperature control was attained through rescaled atom velocities using a weakly coupling thermostat, to keep the macroscopic temperature at the required value of 298 K. To avoid artifacts arising from the classically used Berendsen thermostat, a scaling factor was calculated according to the Berendsen formula from the time average temperature, thereby avoiding use of the strongly fluctuating instantaneous microscopic temperature for velocity rescaling at the individual simulation steps (Zhou & Liu, 2022). Finally, the molecular interactions from eight sampling points within 200 ps following the second cycle were analyzed for all simulation runs (each with n = 4).

2.5. Determination of apparent solubility values

An excess of API was added to the liquid so that a slight residue of particles could be seen suspended at the end of the stirring times. This was mainly due to a paste-like phase separation seen at higher amounts of excess API, creating technical difficulty separating the liquid phase for analysis. Accordingly, a maximum concentration of about 130 mg/mL was used to prepare the samples for which the solubility was studied (using subsequent centrifugation and filtration as described below).

A sample volume of 3 mL with the excess venetoclax was transferred to a 20 mL clear headspace vial of 22.5 x 75 mm (Supelco, Sigma-Aldrich, Steinheim, Germany), sealed using 20 mm aluminum pressure release seals (with PTFE/rubber liner, Supelco, Sigma-Aldrich, Steinheim, Germany) and stirred for 24 h at 350 rpm using a magnetic stirring bar (PTFE-coated, cylindrical with pivot ring, L 12 mm, bar diameter

4.5 mm, BRAND®, Sigma-Aldrich, Steinheim, Germany) on a stirring plate (IKA® RCT basic, Staufen, Germany) at ambient conditions. 2 mL of the sample volume was transferred to a 2 mL safe-lock Eppendorf® tube (Eppendorf AG, Hamburg, Germany) and centrifuged at 14000 rpm for 30 min, in a centrifuge (MPW-65R, MPW Med. Instruments, Warszawa, Poland) with a maximum relative centrifugal force of 20160 x g. A 100 µL sample was then extracted from the supernatant obtained using a positive displacement pipette (Repetman HandyStep®, Gilson, Villiers-Le-Bel, France) with the respective pipette tips (PD-Tips II, Fischer Scientific, Wertheim, Germany) and diluted with a factor of 1:1000 (v/v) in the mobile phase (described in section 2.5.1 below). In case of the long- and short chain triglyceride (sesame oil and Miglyol 812 N) samples, a solvent made of the mobile phase constituents adjusted to 85:15 (v/v) was used in the first round of dilution (with a factor of 1:100) and further diluted to a total factor of 1:1000 using the 70:30 v/v mobile phase. The FeSSIF-V2 (Marques, 2004) (Biorelevant, London, UK) biorelevant media described in section 2.9 was only diluted to 1:100 using the mobile phase. All diluted samples were stirred overnight, after which they were filtered using a 0.45 µm filter (ProFill PA, 0.45 µm, Fisher Scientific, Wertheim, Germany) mounted to 3 mL syringes (Injekt®-F Luer Solo syringe, B. Braun Medical AG, Melsungen, Germany) and filled into amber crimp-top 2 mL HPLC vials (Agilent Technologies Co. Ltd., Beijing, China), sealed with caps (silver, PTFE/silicone septa for 2 mL vials, Agilent Technologies Co. Ltd., Beijing, China) and measured using the method described below (section 2.5.1). The study was performed in three separate sample batches, to make up a triplicate analysis.

2.5.1. Quantification of dissolved API using HPLC

High performance liquid chromatography (HPLC) was used to determine the venetoclax content in the samples. The instrument employed was an Agilent 1100 Series Capillary LC System (Agilent Technologies AG, Basel, Switzerland). The mobile phase consisted of a volumetric ratio of 70:30 of acetonitrile to 10 mM ammonium phosphate buffer (pH 2). A phenyl-hexyl stationary phase of 2.5 µm particle size and 4.6x100 diameter from XSelect® CSH™ (Waters Corporation, Massachusetts, USA) was mounted as the HPLC column. The method was set to sustain a flowrate of 0.5 mL per minute, with detection at an ultraviolet (UV) wavelength of 250 nm, using the Agilent OpenLab software version 3.4 (Agilent Technologies AG, Santa Clara, USA). The retention time obtained was 2.1 ± 0.1 min. The calibration curve was plotted using samples diluted from a stock solution of 1 mg/mL of venetoclax in the mobile phase, to give the concentrations 0.001–0.1 mg/mL. The lower limit of detection (LoD) on the calibration curve was calculated to be 0.004 mg/mL, and the lower limit of quantification (LoQ) on the calibration curve was calculated to be 0.01 mg/mL. The LoD was calculated by dividing the standard deviation of the response by the slope of the standard curve and multiplying the result by 3.3. The LoQ was calculated by multiplying the result of the previously described division by 10 in line with ICH Q2(R1). The analysis was performed in triplicate. The data analysis was performed using the Microsoft Excel data analysis tool pack (version 2016) and GraphPad Prism software (version 10.0.2).

2.6. Dispersion testing and droplet sizes of oil dispersions

The dispersion tests were performed by diluting the samples to 1:100 v/v in demineralized water. The samples were exposed to light shaking (by hand) before the microscopic evaluation performed using polarized optical light microscopy (Model DSX10-SZH, Olympus corporation, Tokyo, Japan). The diameters of 100 of the largest visible spherical droplets were measured in different optical fields and used to plot a distribution. 40x and 100x magnifications were used to study the systems.

2.7. Physical solubility of surfactants in HDES

The physical solubility of the surfactants in HDES was determined by adding 10, 20 and 30 % w/w of the surfactants to the HDES and observing the physical state after 24 h of stirring. If the solution was transparent with no microscopically visible particles after 24 h of mixing at 350 rpm (at ambient conditions), it was deemed dissolved.

2.8. Determination of freezing points using differential scanning calorimetry (DSC)

The freezing points of the samples with and without Tween 80 (10, 20, and 30 % w/w) and 70 mg/mL API were measured by weighing a few milligrams (3–10 mg) of the samples into T_{zero} aluminum pans (TA instruments, Eschborn, Switzerland) sealed using T_{zero} aluminum lids (TA instruments, Eschborn, Switzerland), and exposed to a cooling ramp from 25 °C to −15 °C at 1 °C/min at the nitrogen purge of 50 mL/min on the DSC (Discovery DSC, TA Instruments, Eschborn, Switzerland). The onset point of the exothermic peak was taken as the freezing point of the measured liquids. The analysis was based on the TRIOS software (version 3.1.0.3538) complementary to the Discovery DSC and the study was performed in triplicate.

2.9. USP II dissolution test

A triplicate standard USP II dissolution test was performed using the Pion MacroFLUX™ dissolution instrument (Macroflux™, Pion Inc., Billerica, MA, USA) as a detection device, connected to UV-probes (Pion Rainbow Dynamic Dissolution Monitor®, Pion Inc., Billerica, MA, USA), submerged in the Hanson SR8-Plus dissolution bath (Hanson Research, California, USA). Real-time (on-line) data on the released concentrations of API were displayed on to the AuPRO software version 6.0.3.232, where the data was further analyzed. The dissolution curves were obtained by measuring the concentrations of venetoclax released from 1 mL of 70 mg/mL loaded formulations at the UV-range of 337–357 nm, in 350 mL of FeSSIF-V2, at the stirring rate of 75 rpm and temperature of 37 °C over the course of 2 h. Note that the formulations tested were prepared fresh and used within 24 h of production. FeSSIF-V2 was prepared according to instructions provided on the biorelevant homepage (biorelevant.com) (Marques, 2004) using a standard phosphate buffer base adjusted to pH 6.5 with 0.1 M sodium hydroxide (Sigma-Aldrich, Steinheim, Germany). The standard curve was determined based on a stock solution of 1 mg/mL of venetoclax in a solution of 10:90 v/v of glacial acetic acid to acetonitrile, at concentration ranges of 2–40 µg/mL diluted in FeSSIF-V2. The apparent supersaturations were then presented by dividing the API concentration obtained at 120 min of release by the solubility of venetoclax in FeSSIF-V2.

2.10. Stability test − chemical degradation of venetoclax

A triplicate stress test was performed in three batches of each formulation to evaluate the stability of the HDES with 10, 20 and 30 % w/w of added Tween 80 versus the pure HDES. The API loadings corresponded to 70 mg/mL in all formulations. A volume of 1 mL was transferred to a clear crimp-top hermetically sealed HPLC glass vial (ALWCSI Technologies Co. Ltd., Zhejiang PR, China), sealed using silver rubber-septa crimp caps (ALWCSI Technologies Co. Ltd., Zhejiang PR, China), and placed in the study condition of 60 % relative humidity (RH) at 25 °C. The humidity was controlled using saturated salt desiccators of sodium bromide (57.6 % RH) placed in jars positioned in temperature-regulated humidity chambers (Memmert GmbH + Co. KG, Schwabach, Germany). The peak signal corresponding to the API was obtained using HPLC (section 2.5.1) and compared at two time-points: the initial time-point before starting the stress test and the second point after 2 weeks of stressing. The chromatograms were also monitored for the appearance of additional peaks. Variations in the retention time of API-related peaks

were accepted up to ± 10 %. Additionally, the samples were also studied for traces of crystallinity using microscopy (Model DSX10-SZH, Olympus corporation, Tokyo, Japan).

2.11. Statistical analysis and graphics using GraphPad Prism

All statistical analyses were performed using GraphPad Prism (version 10.0.2, GraphPad software, California, USA). The one-way ANOVA calculations were complemented with either Tukey or Dunnett tests where necessary. The Tukey test was employed when the ANOVA test compared different sets of means to each other, whilst the Dunnett test was applied when the sets of means were to be compared to a single mean value. The null hypotheses in the statistical tests presumed that the means of two or more populations are equal, with a variation threshold (*p*-value) of 0.05. *P*-values below 0.05 resulted in the rejection of the null-hypothesis, demonstrating a significant difference amongst a group of means.

All graphs and figures of the results obtained from all experiments were also illustrated using the GraphPad prism program.

3. Results

The results section is divided into three main parts: 3.1, 3.2, and 3.3. The first section characterizes the HDES itself with a model of its phase behavior. This section concludes by studying venetoclax solubility in HDES as compared to other lipophilic media and analyses the mixtures' molecular architecture with and without drug using molecular dynamics (MD) simulations. Section 3.2 is about the impact of adding surfactant (i.e., Tween 80) to the DES to study the performance of the final lipid-based formulation. Finally, based on the findings in 3.2, an arbitrary loading concentration was then used to characterize the dissolution of API from the formulations using the in-vitro USP II dissolution setup.

3.1. HDES selection, characterisation, optimization, and API solubility

The HDES used in this study has been previously described outside the field of pharmaceutics by Florindo et al., 2018 as a liquid used for extracting bisphenol A (a micropollutant) from aqueous environments (Florindo et al., 2018). The HDES is made of a 1:2 M ratio of dodecanoic acid to decanoic acid (Florindo et al., 2018). It can be seen in Fig. 1 showing a clear homogenous liquid with the melting point of 19.70 °C ± 0.11 °C, viscosity of 9.3 ± 0.3 mPa•s, density of 896.0 ± 0.1 kg/m^3 and a water content below 0.07 % w/w. Dodecanoic acid (DoA) and decanoic acid (DeA) have both been defined as pharmaceutically safe excipients, used for taste masking, emulsification, food additives, lubricants or surfactants (Rowe et al., 1994). They are both medium-chain saturated fatty acids, with a chain length of 10 carbons in the case of the decanoic acid and 12 carbons in the dodecanoic acid (Rowe et al., 1994).

3.1.1. HDES characterization

The selected HDES is characterized using phase diagrams to establish the thermodynamic behavior of the liquid. The ideal phase behavior was assessed using the Schröder van Laar (SvL) equation (equation (1) with the activity coefficient of unity) together with a solid–liquid line (SL-line) including UNIFAC activity coefficients (equation (1), referred to as the UNIFAC model. Finally, the experimentally obtained solid–liquid line can be found overlaid in Fig. 2. The resulting eutectic points from Fig. 2 are reported in Table 1 with fusion properties taken from the literature. The melting point of the DeA was set to 31.5 °C (Hawley & Lewis, 2002), with an enthalpy of fusion of 29.4 kJ/mol (Moreno et al., 2007). The melting point for DoA was found to be 43.2 °C (Jiesheng et al., 2016) and the enthalpy of fusion to be 36.7 kJ/mol (Moreno et al., 2007). These values were used to plot the modelled systems, i.e., the ideal SvL and the UNIFAC model.

The eutectic point in the ideal SvL system was only 1.12 °C higher than that found by the DSC experiments. The UNIFAC model resulted in a eutectic temperature only 0.03 °C lower than the SvL value and was thus closer to the actual experimental value of 19.70 °C ± 0.11 °C. Accordingly, the UNIFAC model results in a DeA molar fraction around 0.05 units lower than the experimental molar fraction at the eutectic point. Hence, the SvL molar fraction obtained at 0.02 units lower than the experimental molar fraction, was closer to the experimentally

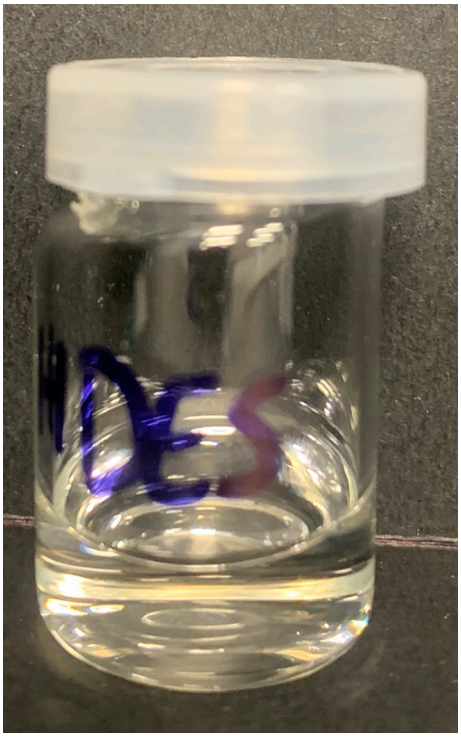

Fig. 1. Pure hydrophobic deep eutectic solvent (HDES), made of decanoic acid and dodecanoic acid at the molar ratio of 2:1.

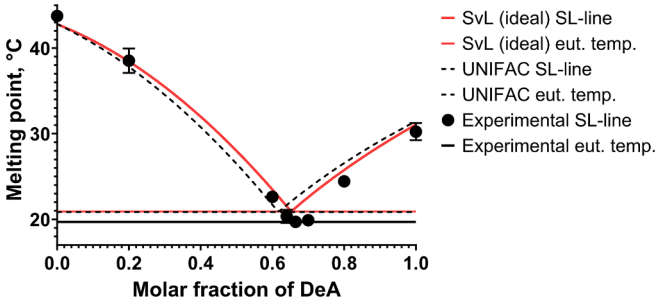

Fig. 2. Modelled solid–liquid lines (SL-line) and eutectic temperatures (eut. temp.) found through melting points calculated by the Schröder van Laar (SvL) equation, consideration of UNIFAC activity coefficients in equation (1), overlaid with the experimental thermoanalytical values (n = 3, mean ± SD).

Table 1
Summary of eutectic points obtained from the modelled phase diagrams of Schröder van Laar solid–liquid line (activity coefficient of unity) and the modelled UNIFAC activity coefficients in equation (1) with experimental values obtained from DSC (n = 3, mean ± SD).

Model	Eutectic point	
	Molar fraction, DeA:DoA	Temperature
Schröder van Laar (ideal)	0.65:0.35	20.82 °C
UNIFAC	0.62:0.38	20.79 °C
Experimental	0.67:0.33	19.70 °C ± 0.11 °C

obtained eutectic point (2:1 of DoA to DeA). Collectively the results and the UNIFAC approximation agree in that no substantial deviance from ideal mixing behavior was obtained.

3.1.2. Optimization of HDES as a lipid-based formulation (LBF)

The HDES showed highly hydrophobic characteristics as it did not spontaneously form droplets upon dispersion in an aqueous medium. This can be seen in Fig. 3, showing a droplet of HDES floating on top of the aqueous liquid.

To improve dispersion of HDES into water, several surfactants were examined. The surfactants were assessed at the concentration of 10, 20, and 30 % w/w of the HDES, as described in section 2.7. The surfactants tested included Labrasol ALF (PEG-8 capric glycerides), Labrafil M 2125 CS (corn oil PEG-6 esters), Labrafac lipophile WL 1349 (medium-chain TGs), Tween 80 (polysorbate 80), Gelucire 44/14 (lauroyl PEG-32 glycerides), Gelucire 48/16 (PEG-32 stearate), Soluplus®, and Poloxamer 188, of which only the first four were soluble at these concentrations. These surfactants were then selected for further testing and evaluation of aqueous dispersibility. The dispersibility of the prepared mixtures of HDES with either Labrasol ALF, Labrafil M 2125 CS, Labrafac lipophile WL 1349, or Tween 80 at the concentrations of 10, 20 and 30 % w/w were tested in aqueous medium according to the method described in section 2.6. They all resulted in coarse emulsions upon dispersion and light shaking. The average droplet diameters of the evaluated dispersions are outlined in Table 2.

The data was analyzed with statistical one-way ANOVA Dunnett testing, comparing droplet diameters of the surfactant-containing samples to those of the pure HDES with an average droplet diameter of 78.3 μm ± 24.7 μm. Accordingly, samples with Tween 80 (polysorbate 80) were the only ones resulting in a significant drop in droplet diameter.

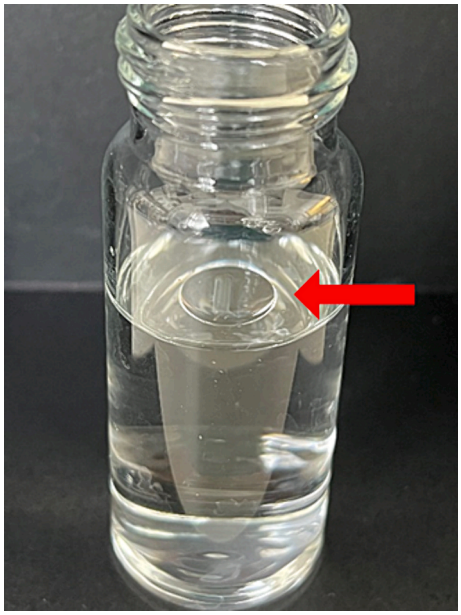

Fig. 3. Pure HDES dispersed in water at 1:100 v/v. Arrow pointing at the floating droplet of the HDES on top of the water.

Therefore, HDES with either 10, 20, or 30 % w/w of Tween 80 were selected as the final LBF candidates. These all had a homogenous and transparent appearance.

3.1.3. Addition of API to HDES

Venetoclax solubility in the functional samples was determined according to the methods described in section 2.5. It is noteworthy that adding a large excess of venetoclax typically changed the HDES liquid samples into a paste by the end of the 24 h equilibration time. Hence, a trial-and-error method was applied to target an excess concentration of venetoclax that would leave behind only a small residual amount of dispersed API particles in the vials at the end of equilibration. The solubility values obtained were then compared to those found in a long-chain triglyceride oil (sesame oil), a medium-chain triglyceride (Miglyol® 812 N) and FeSSIF-V2. The selected oils were to represent other classically used API-carrying oil phases in LBFs to have a solubility reference. Table 3 shows that increased amounts of venetoclax can be dissolved in the HDES compared to the reference oils tested. Nevertheless, the solubility of venetoclax was higher in all the oils compared to the aqueous FeSSIF-V2 medium, which showed a solubility value below the LoQ described in section 2.5.1. Based on the substantial solubility improvement in the chosen HDES of DeA:DoA (2:1) compared to the other two oils (i.e., sesame oil and Miglyol® 812 N), this new type of LBF was further investigated.

3.1.3.1. Mechanistic study on molecular positioning of venetoclax in HDES. Molecular dynamics (MD) simulations were performed on the pure HDES (DeA:DoA at the molar ratio of 2:1) and the HDES with 5 % w/w of venetoclax, to study the molecular architecture of the formulation mechanistically (see Fig. 4). The average molecular interactions of the quadruplicate simulation runs are reported in Table 4.

The simulation showed that in total there were around 150–160 accepted and donated hydrogen bonds and about 12′000 hydrophobic contact points between the pure HDES components. Once 5 % w/w of venetoclax was added, these values were reduced to about 130–140 accepted hydrogen bonds and 140–150 donated hydrogen bonds, resulting in ~ 11′000 hydrophobic contact points between the constituting components (DeA and DoA) in the entire simplified model system. Furthermore, a statistical analysis comparing the mean hydrogen bonding energies between the DeA and DoA molecules showed a notable reduction (p-value < 0.0001) in the case of the venetoclax-containing sample versus the pure HDES, going from 7179.1 kJ/mol in the pure HDES to 6195.0 kJ/mol in the HDES loaded with 5 % w/w of venetoclax. The API showed a slight preference for interactions with the DeA component compared to the DoA component, as slightly higher hydrogen bonding and hydrophobic energies were observed between

Table 3
Solubility of venetoclax in HDES versus other media, including sesame oil (long chain triglyceride), Miglyol® 812 N, and FeSSIF-V2 (n = 3, mean ± SD).

Solubilising medium	Venetoclax solubility at 25 °C after 72 h
HDES (DeA:DoA, 2:1)	118.2 ± 4.3 mg/mL
Sesame oil	5.3 ± 0.1 mg/mL
Miglyol® 812 N	1.30 ± 0.01 mg/mL
FeSSIF-V2	< LoQ ($9.4 \bullet 10^{-3} \pm 0.6 \bullet 10^{-3}$ mg/mL)

Table 2
Overview of the droplet diameters of the HDES with 10, 20, and 30% w/w of the different surfactants.

Surfactant concentration	Droplet diameter, μm			
	Labrafac lipophile WL 1349	Labrafil M 2125 CS	Labrasol ALF	Tween 80
10 % w/w	86.7 ± 54.7	44.2 ± 18.0	47.8 ± 31.4	12.4 ± 5.6
20 % w/w	86.2 ± 30.7	42.0 ± 18.1	36.3 ± 13.2	7.4 ± 1.7
30 % w/w	73.0 ± 41.1	58.7 ± 24.1	32.5 ± 9.7	9.5 ± 4.1

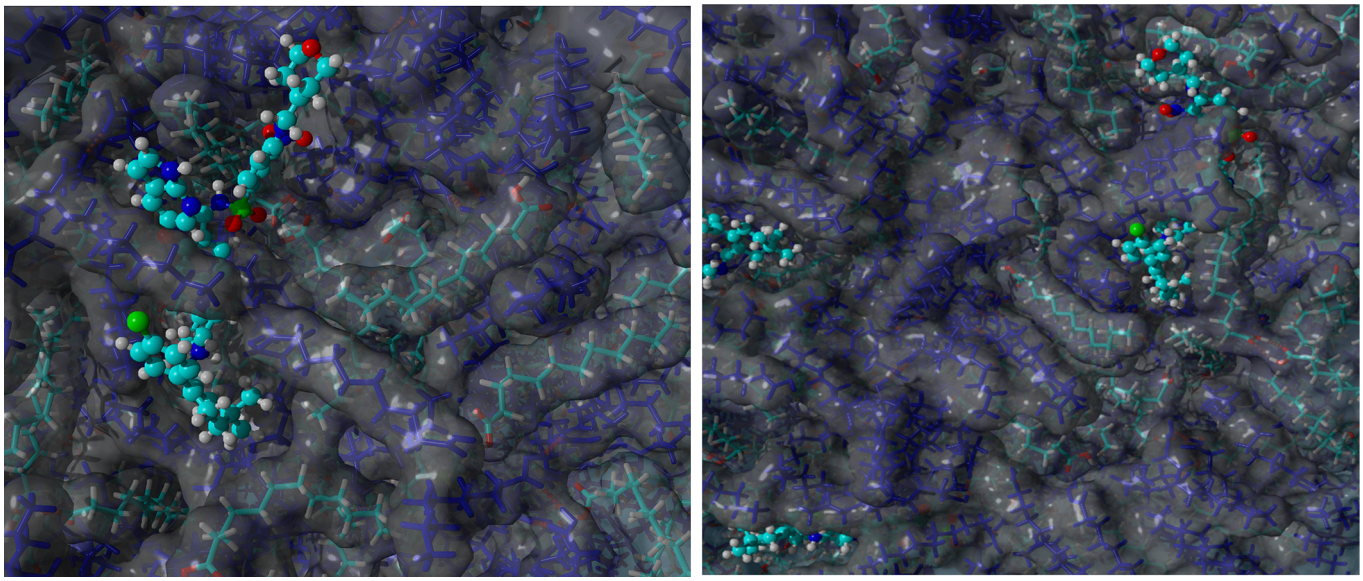

Fig. 4. Snapshot images following equilibration at room temperature HDES components are depicted as tubes- and API as ball-and-stick model. The tubes model shows DeA acid in blue, whilst the DoA is given without altered standard colors (i.e., turquoise for carbons). The molecular surface of the DES components is shown in both images to mark the solubilizing environment of the API. (For interpretation of the references to colour in this figure legend, the reader is referred to the web version of this article.)

Table 4
Overview of interaction energies obtained through the 200 ps sampling at 298 K (second cycle) simulations in samples with 5 % w/w API versus the interaction between the DeA and DoA in the pure HDES (without API) shown in the first row (n = 4, mean ± SD).

Interaction type	Molecular interaction energies, kJ/mol			
	Hydrogen bonding	Hydrophobic	Pi-Pi	Cation-pi
DeA with DoA (without API)	7179.1 ± 283.9	9454.0 ± 79.3	–	–
DeA with DoA (with 5 % w/w API)	6195.0 ± 514.1	9021.7 ± 330.6	–	–
DeA with API	549.7 ± 50.4	811.7 ± 73.4	–	–
DoA with API	263.9 ± 24.0	430.6 ± 40.0	–	–
API with API	117.2 ± 16.7	326.4 ± 24.1	52.9 ± 9.1	24.9 ± 6.4

the DeA with API (549.7 kJ/mol and 811.7 kJ/mol) as opposed to the DoA with API (263.9 kJ/mol and 430.6 kJ/mol) (p-value < 0.0001). In the entire simulated system, DeA and venetoclax showed around 13 accepted and 16 donated hydrogen bonds with roughly 1000 hydrophobic contacts, whereas the DoA and venetoclax had about 4 accepted and 8 donated hydrogen bonds and of the order of 500 hydrophobic contacts. The API also revealed some interactions with itself through hydrogen bonds, pi-pi interactions, and cation pi interactions. However, these values were found to be substantially lower than the interaction energies occurring between the API and the DES components. The distribution of API appeared to be comparatively homogenous in the model system indicating good solubilization without signs of phase separation from either the drug or any other HDES component.

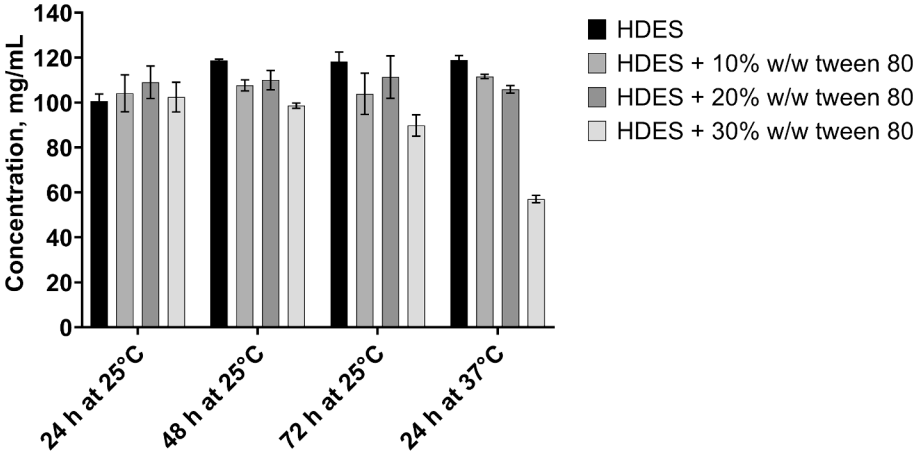

Fig. 5. Bar chart of venetoclax solubilities (mg/mL) in HDES and HDES with 10, 20, and 30 % w/w Tween 80 at 25 °C after 24, 48 and 72 h and 37 °C after 24 h (n = 3, mean ± SD).

Table 5
Overview of venetoclax solubilities (mg/mL) in HDES and with added 10, 20, and 30 % w/w Tween 80 at 25 °C after 24, 48 and 72 h and 37 °C after 24 h (n = 3, mean ± SD).

Venetoclax solubility (mg/mL) in the LBF mixtures				
Formulation	**25 °C 24 h**	**25 °C 48 h**	**25 °C 72 h**	**37 °C 24 h**
HDES	100.6 ± 3.2	118.7 ± 0.7	118.2 ± 4.3	118.9 ± 2.0
HDES + 10 % w/w Tween 80	104.1 ± 8.2	107.6 ± 2.5	103.9 ± 9.2	111.6 ± 1.0
HDES + 20 % w/w Tween 80	109.0 ± 7.2	110.0 ± 4.3	111.3 ± 9.5	105.9 ± 1.7
HDES + 30 % w/w Tween 80	102.5 ± 6.6	98.6 ± 1.2	89.8 ± 4.8	57.1 ± 1.7

3.2. Impact of Tween 80 on LBF drug solubility and release

3.2.1. Impact of Tween 80 on drug solubility in the formulation

The solubility of venetoclax in the final formulation candidates was determined and compared to the pure HDES as depicted in Fig. 5 and listed in Table 5. To assess the equilibration time, statistical evaluations of each of the formulations were performed using Tukey and Dunnett ANOVA tests (section 2.11). Thus, after 72 h of stirring at 25 °C, equilibrium was reached except for the 30 % w/w Tween 80, which varied significantly from the values obtained at 24 and 48 h at 25 °C. A reduction from 118.2 ± 4.3 mg/mL in HDES to 89.8 ± 4.8 mg/mL in the 30 % w/w Tween 80 sample was observed in the 72 h equilibrated samples. Based on the data obtained, the final formulations were loaded with 70 mg/mL of API, representing an arbitrarily selected dose strength corresponding to a drug-loading of 7.2 % w/w in the pure HDES, 6.6 % in the HDES formulation with 10 % w/w Tween 80, 5.9 % w/w in the HDES with 20 % w/w Tween 80, and 5.2 % w/w in the HDES with 30 % w/w Tween 80.

3.2.2. Impact of venetoclax on dispersibility of HDES with Tween 80

The impact of the added venetoclax on droplet diameter was studied in the LBF formulations in absence and presence of different Tween 80 concentrations (Table 6). In the case of the formulations containing Tween 80, adding venetoclax changed the droplet-diameter reducing effect of the added surfactant, as described in section 3.1.2. The droplet diameter changed to values comparable to that of the pure HDES with API, and only the HDES with 30 % w/w Tween 80 resulted in a smaller droplet size.

3.2.3. Impact of Tween 80 and venetoclax on the freezing point of HDES

The freezing points were studied because the eutectic point of the DeA:DoA (2:1) HDES was 19.7 °C ± 0.1 °C, and hence could crystallize at ambient conditions (Palmelund et al., 2020). The acquired values are summarized in Table 7.

The addition of 10, and 20 % w/w Tween 80 did not significantly change the freezing point; a drop from 17.3 °C ± 0.1 °C in the pure HDES to 15.4 °C ± 0.7 °C in HDES with 30 % w/w of Tween 80 was observed. An additional drop in the freezing point was observed once the API was added to the formulations of 20 and 30 % w/w Tween 80, resulting in a difference of −1.8 °C and −3.1 °C respectively compared to the HDES with API.

3.2.4. Impact of Tween 80 on preliminary stability testing of the formulations

The stability of the samples was determined according to the method described in section 2.10. As presented in Fig. 6, the concentration of the API in the stressed samples of 30 % w/w Tween 80 deviated significantly after two weeks of storage. However, no other peak was observed on the chromatograms, and the retention time of the API-corresponding peak did not deviate. Additionally, no precipitates were observed microscopically after the two-week stressing cycle.

Table 6
Change in droplet diameter in the formulations with and without API (n = 3, mean ± SD).

Formulation	**Droplet diameter, µm**	
	without API	**with 70 mg/mL API**
HDES	78.3 ± 24.7	45.5 ± 33.5
HDES + 10 % w/w Tween 80	12.4 ± 5.6	44.1 ± 29.8
HDES + 20 % w/w Tween 80	7.4 ± 1.7	48.2 ± 28.7
HDES + 30 % w/w Tween 80	9.5 ± 4.1	33.9 ± 17.5

Table 7
Overview of freezing points of the HDES with 10, 20, 30 % surfactant, with and without 70 mg/mL of venetoclax (n = 3, mean ± SD).

Formulation	**Freezing point, °C**	
	without API	**with 70 mg/mL API**
HDES	17.3 ± 0.1	16.8 ± 0.4
HDES + 10 % w/w Tween 80	18.0 ± 0.1	16.0 ± 0.6
HDES + 20 % w/w Tween 80	17.2 ± 0.4	15.0 ± 0.4
HDES + 30 % w/w Tween 80	15.4 ± 0.7	13.7 ± 0.4

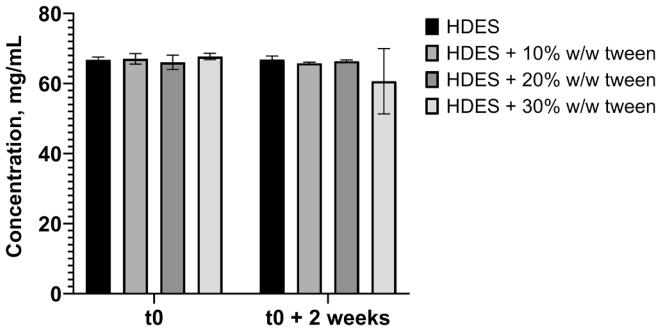

Fig. 6. Change in the concentration of API in stressed samples at the initial time point (t0) and after two weeks (t0 + 2 weeks). Values are representative of the concentration change (chemical degradation) of the API in the samples (n = 3, mean ± SD).

3.3. In-vitro dissolution assessment using the USP II setup

The dissolution profiles of the prepared formulations, namely the pure HDES and HDES with 10, 20, and 30 % w/w Tween 80, with API-loading of 70 mg/mL can be seen in Fig. 7. The figure shows higher concentrations released from the samples with higher concentrations of Tween 80. The concentrations of API released after 120 mins of dissolution are summarized in Table 8.

The surfactant enabled apparent supersaturation of API in the release medium, FeSSIF-V2. Apparent supersaturations of 1.7, and 2.6 were seen for the 10 % and 20 % w/w Tween 80 samples, whilst apparent supersaturations up to 3.1 were recorded for the HDES with 30 % w/w Tween 80. A lower apparent supersaturation of 1.1 was documented in the pure HDES. The difference between each of the estimated supersaturation values diminished with increasing Tween 80 concentrations, therefore a limit of supersaturation was apparently given for increased surfactant concentrations.

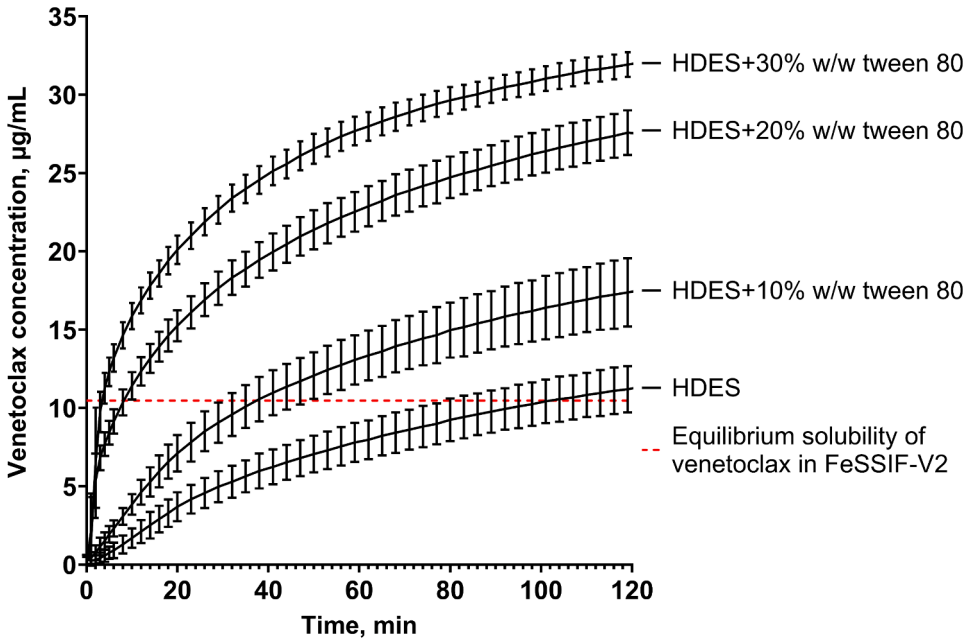

Fig. 7. In-vitro USP II dissolution concentrations of 70 mg venetoclax from 1 mL of DeA:DoA (2:1) (HDES), and HDES with 10, 20, and 30 % w/w of Tween 80 in 350 mL FeSSIF-V2, at 37 °C over 120 min (n = 3, mean ± SD). The red dashed line refers to the equilibrium solubility of venetoclax in FeSSIF-V2. (For interpretation of the references to colour in this figure legend, the reader is referred to the web version of this article.)

Table 8
Overview of dissolved concentration of venetoclax recorded at 120 min (n = 3, mean ± SD).

Formulation	Concentration of dissolved API, µg/mL
HDES	11.3 ± 1.5
HDES + 10 % w/w Tween 80	17.5 ± 2.2
HDES + 20 % w/w Tween 80	27.5 ± 1.4
HDES + 30 % w/w Tween 80	32.0 ± 0.8

4. Discussion

4.1. Utilization of HDES to formulate a highly lipophilic model compound

The scientific study of DES has been a thriving field in chemistry for a few years, but only in recent years have these systems sparked a rising interest in delivering nutraceuticals and drugs (Faggian et al., 2016; Fourmentin et al., 2021; Palmelund, Eriksen, et al., 2021; Panbachi et al., 2023; Sut et al., 2017). A seminal study compared drug solubility in different DES with values obtained in common pharmaceutical solvents (Palmelund et al., 2019). The authors found a range of different solubility values, some impressively high, but it was the specific chemistry of both vehicle and API that determined the extent of drug solubilization. It seems that much pharmaceutical novelty still remains to be uncovered and a recent example is the embedding of a polymeric-precipitation inhibitor in a DES to obtain sustained drug supersaturation values on aqueous dispersion of the formulation (Panbachi et al., 2023). For the present work, hydrophobic systems, HDES were to be explored to formulate the highly lipophilic model drug venetoclax. Although eutectic mixtures and DES have been used in chemical engineering before (Florindo et al., 2018), a pharmaceutical application to formulate a poorly water-soluble drugs are new to the best of our knowledge. Part of the research question was to study such an HDES starting from the phase diagram to the drug solubilising potential. A further aim was to get molecular insights into the structure of such a system. Moreover, there was the biopharmaceutical perspective on how such a system would disperse in aqueous medium and eventually add a surfactant, which would provide a new kind of LBF with an HDES replacing a more traditional oily phase composed of glycerides.

4.2. In-silico versus experimental characterization of the HDES

A majority of early published studies on DES presented formulations without investigating their phase behavior. As a result of the present study, the thermodynamically non-ideal behavior of the HDES was confirmed through a lower observed eutectic point compared to that obtained in the modelled 'ideal' mixture following the Schröder van Laar equation (SvL), as displayed in Fig. 2. The DeA:DoA (2:1) system has previously been reported as a hydrophobic DES (HDES) in the work of Dwamena, 2019, yet the phase diagram presented in the present pharmaceutical study aimed to provide a deeper thermodynamic understanding of the system. The overall proximity of the computationally predicted ideal eutectic point to the experimental eutectic point could imply that the HDES behaved rather as a eutectic mixture instead of a true 'deep' eutectic mixture. However, in the definitions of DES in the literature there is no clear threshold for the magnitude of negative deviation of the eutectic point from ideal behavior (Abranches & Coutinho, 2023; Hansen et al., 2021; Martins et al., 2019). The term DES or HDES is often broadly used in applied sciences without knowledge of comparative ideal phase behavior; in the present study, the 1.12 °C lower experimental eutectic point was identified and the DeA:DoA (2:1) was called a HDES in line with the pioneering work Florindo et al., 2018.

As for the prediction of DES behavior, the UNIFAC model performed similar to the SvL model, predicting a eutectic temperature only 0.03 °C closer to the experimental value. However, the SvL model predicted a molar fraction that was slightly closer to the experimental molar fraction. Despite the eutectic melting values being very similar to the experimental output, the UNIFAC model was apparently not much more accurate than the ideal SvL approach for the system studied. Overall, the precision of both models can be viewed as acceptable. There are possible small errors from the fusion data obtained from the literature and on the other hand, there is also the possibility that small experimental errors occurred. Finally, pioneering work on UNIFAC modelling of therapeutic DES already indicated that model precision depended to some extent on the specific system studied. While the model precision in the present study was adequate for the purpose of characterizing a fatty acid

mixture, a main drawback of UNIFAC modelling is generally the availability of group contributions and all possible interaction terms, which generally limits current UNIFAC modelling of complex APIs.

The modelling of the phase diagram was complemented with MD simulations to gain atomistic insights into the structure of the DES both as binary mixture of the fatty acids as well as in the presence of the model drug venetoclax. The simulations were based on an all-atom force field (GAFF2) (Wang et al., 2004) of the AMBER family of potential energy functions. This type of force field has often been used to model DES as a recent review indicated (Tolmachev et al., 2022). As a snapshot result of the equilibration cycle at room temperature, Fig. 4 reveals a structure in accord with the more recent view of DES as a chaotic 'hydrogen bond-alphabet-soup' (Ashworth et al., 2016). Moreover, such high configuration randomness has also been observed in previous MD DES simulations (Ashworth et al., 2016; Fourmentin et al., 2021). Since the prepared HDES is made of fatty acids, a possible expectation was some laminar layering of the alkyl chains to occur, as typically observed in fatty acid co-crystals (Prathapa et al., 2018). However, Fig. 4 shows no traces of such ordered macrostructural configuration of the liquid. Thus, the chaotic liquid structure of the DES was apparently favorable for the two constituting components to achieve a high configurational entropy contribution to the free energy of mixing.

As a result of added API, a decline in the occurrence of hydrogen bonds between the HDES components (DeA and DoA) was observed. Venetoclax further decreased the hydrophobic interactions of the interacting fatty acids (Table 4) so the presence of this external component in the HDES caused a moderate perturbance of the system. It is noteworthy in this context that the solubility reported in this study is an 'apparent' solubility value. This is because excess venetoclax within the system caused the liquid mixture to morph into a coarse paste-like material. Since the solubilization of the APIs in DES systems are dependent on the hydrogen-bond network within the DESs, it is critical that the DES itself can sustain a sufficiently strong hydrogen bonding network in the presence of the API (Palmelund et al., 2020). Therefore, an apparent maximum solubility may represent a limiting drug concentration at which the DeA:DoA (2:1) HDES still has the capacity to sustain structural intactness.

Apparently, drug solubilization of the HDES relies on the hydrogen bonds in the system where some bonds with drug are often favorable regarding solvation capacity but the network of such interactions between the DES components should not be overly interrupted. Accordingly, good DES formulations are based on finely balanced interactions and the case of venetoclax apparently showed more hydrophobic interactions than hydrogen bonding with the DES components. The drug was interacting on the average slightly more with the DeA than the DoA component, but this was likely due to the shorter chain length of DeA resulting in a higher density of carboxylic groups to interact. Venetoclax was further shown to interact with itself occasionally via hydrogen bonds, hydrophobic interactions, pi-pi interactions, and proton-pi interactions. That said, due to the much lower number of drug molecules in the simulation as compared to DES components, these findings were not evaluated quantitatively and should be regarded as qualitative information. This self-cohesion tendency of venetoclax underlines the importance of excipient interactions, even more important for such a hydrophobic compound in an aqueous environment on dispersion to keep the drug from precipitation (Koehl et al., 2021).

4.3. Use of the HDES as oil phase in lipid-based system

As described in the introduction, venetoclax is a BCS class IV API, not meeting the requirements of Lipinski's rule of 5 (Hartung et al., 2023). The high lipophilicity of venetoclax comes with a problematically high crystal energy (Koehl et al., 2021) making drug solubility even in hydrophobic solvents rather limited, which has led to previous consideration of lipid-based suspension formulations and lipophilic salts (Koehl et al., 2021, 2022). The present study interestingly revealed about a 100-fold increased solubility in the DeA:DoA (2:1) HDES compared to that in sesame oil and Miglyol® 812 N. The latter two oils represent other classically employed long- and medium-chain triglycerides in LBFs to solubilize API. Hence, a substantial solubility improvement was attained compared to standard lipid phases for LBF, which raises the question of whether the designation of the current system as a true DES or just a eutectic mixture has any relevance from a practical pharmaceutical perspective. Thus, the selected HDES offers a successful replacement for such oils as higher amounts of API could be solubilized in the DES vehicle.

As LBF have to disperse adequately in the gastrointestinal tract (Porter et al., 2008), initial aqueous dispersibility testing was conducted. Tween 80 was added to the HDES vehicle as a surfactant at the concentrations of 10, 20, and 30 % w/w. The addition of the surfactant from the group of PEGylated sorbitan esters significantly reduced the droplet diameter in comparison to other surfactants (refer to Table 2) in an aqueous 1:100 v/v dispersion. The resulting emulsion can justify calling the initial surfactant containing HDES a self-emulsifying drug delivery system (SEDDS) (Feeney et al., 2016). As the composition of this type of system is new, there is no clear category assignment for the lipid formulation classification system (Feeney et al., 2016; Pouton, 2006). Following the addition of surfactant, the intactness of the solubilization capacity of the formulation was re-examined. Indeed, higher amounts of the surfactant, specifically 30 % w/w of Tween 80, resulted in comparatively lower solubilization of venetoclax in the formulations. This is mainly because higher amounts of Tween 80 leave little compositional space for the HDES in the given volume of the formulation. As a result, lower solubility was observed due to less of the main solubilizing component that was apparently the HDES. This could also explain the deviation in venetoclax concentrations recorded in the stressed HDES samples with 30 % w/w tween, indicating a potential start of nucleation of a solid component.

In contrast to the lower API solubilization in the formulations, the higher concentrations of incorporated Tween 80 resulted in higher concentrations of venetoclax released into the aqueous medium (FeSSIF-V2) during the in-vitro release test (refer to Fig. 7). Specifically, the dissolution of API from the HDES with 30 % w/w Tween 80 was the highest compared to the rest of the samples. The venetoclax concentration released from the Tween 80-containing formulations into the FeSSIF-V2 dissolution medium clearly exceeded the equilibrium concentration in pure medium, leading to apparent drug supersaturation. An apparent supersaturation based on the biorelevant solubility can provide first estimates of a final supersaturation in the release medium that may be also influenced by the highly diluted excipients in the medium. In the present case, the latter possible solubility effect is further diminished by a fast absorption of the fatty acids in vivo.

Apparent supersaturation is also often observed with other LBFs (Kuentz, 2019), as it is triggered by fast dispersion and hence a partition process. The smaller droplets or even colloids would result in enhanced release through increased surface area to volume fractions of the formed droplets. It was interesting to observe that the impact of surfactant concentration on droplet diameter was greatly affected by adding venetoclax. The high lipophilicity of the venetoclax apparently altered the formulation's hydrophilic-lipophilic balance (HLB), causing a change in diameter of the dispersed droplets (Wang et al., 2023). The 30 % w/w Tween 80 addition to HDES still resulted in slightly smaller droplet sizes compared to the pure HDES with venetoclax but the effects of the surfactant in reducing specific surface energy to promote dispersion were clearly limited by the presence of drug. Although formulators generally target small droplet sizes on dispersion, one has to add that there are no clear targets in what is desirable to achieve (Feeney et al., 2016). Thus, improving a poorly dispersible oil phase by adding a surfactant is most likely beneficial from a biopharmaceutical perspective. However, surfactant addition must be balanced; it should not displace too much of the HDES in a composition to still achieve excellent drug solvation capacity, as obtained in this study.

5. Conclusion

This study introduced a novel DES-based oil-phase for application in lipid-based formulations. The selected DES was an HDES made of decanoic- and dodecanoic acid in the molar ratio of 2:1. This HDES resulted in a eutectic temperature of 19.70 °C ± 0.11 °C and the mixture dissolved an unprecedented amount of 118.2 ± 4.3 mg/mL of the highly lipophilic drug venetoclax. The HDES performed 100-times better than the long- and medium chain triglycerides sesame oil and Miglyol® 812 N in terms of solubilization. The formulation was then optimized for better aqueous dispersion using Tween 80 as surfactant in different concentrations. Although the surfactant concentration of 30 % w/w affected the solubilization capacity, no other significant change in the overall characteristics of the HDES was observed. The formulation was finally in-vitro tested using a compendial USP II release test where the resulting concentrations indicated that the surfactant increased the released concentrations past the equilibrium concentration of the API in the dissolution medium. Future biopharmaceutical testing may consider the separate steps of gastric and intestinal release. Further testing under lipolysis conditions is an option but only the surfactant can undergo lipolysis in the present case (Arnold et al., 2012). There is surely more research in this field to be done but the present study already suggests that using an HDES as lipophilic phase for LBF is a pertinent new drug delivery approach. The high solvation capacity of HDESs observed is highly encouraging for any further studies with LBFs to tackle the poor solubility of biopharmaceutically challenging APIs.

CRediT authorship contribution statement

Shaida Panbachi: Writing – original draft, Visualization, Validation, Project administration, Methodology, Investigation, Formal analysis, Data curation, Conceptualization. **Josef Beranek:** Writing – review & editing, Supervision, Resources, Conceptualization. **Martin Kuentz:** Writing – review & editing, Supervision, Resources, Conceptualization.

Declaration of competing interest

The authors declare that they have no known competing financial interests or personal relationships that could have appeared to influence the work reported in this paper.

Data availability

Data will be made available on request.

Acknowledgments

The author would like to thank the invaluable assistance and cooperation of Martina Nehls, Laura Billingham, and Elilaha Sivasubramaniam on their valiant efforts and input in the development of the excel file for modelling, and the screening and characterization of the initial HDES prototypes. Andrew Brown is also acknowledged for his valued proof-reading of the manuscript.

Funding and role of funding source

This work has received funding from the European Union's Horizon 2020 research and innovation program the Marie Skłodowska-Curie grant agreement No 955756. (InPharma). The funding source was not involved in the study design, in the collection, analysis and interpretation of data, in the writing of the report, nor in the decision to submit the article for publication.

References

Abdelquader, M.M., Li, S., Andrews, G.P., Jones, D.S., 2023. Therapeutic deep eutectic solvents: A comprehensive review of their thermodynamics, microstructure and drug delivery applications. Eur. J. Pharm. Biopharm. 186, 85–104. https://doi.org/10.1016/J.EJPB.2023.03.002.

Abranches, D.O., Coutinho, J.A., 2023. Everything you wanted to know about deep eutectic solvents but were afraid to be told. Annual Review of Chemical and Biomolecular Engineering 14 (1), 141–163. https://doi.org/10.1146/annurev-chembioeng.

Abranches, D.O., Martins, M.A.R., Silva, L.P., Schaeffer, N., Pinho, S.P., Coutinho, J.A.P., 2019. Phenolic hydrogen bond donors in the formation of non-ionic deep eutectic solvents: The quest for type V DES. Chem. Commun. 55 (69), 10253–10256. https://doi.org/10.1039/C9CC04846D.

Abusleme, J.A., Vera, J.H., 1985. The quasi-chemical group solution theory for organic mixtures. Fluid Phase Equilib. 22 (2), 123–138. https://doi.org/10.1016/0378-3812(85)85015-9.

Arnold, Y.E., Imanidis, G., Kuentz, M., 2012. In vitro digestion kinetics of excipients for lipid-based drug delivery and introduction of a relative lipolysis half life. Drug Dev. Ind. Pharm. 38 (10), 1262–1269. https://doi.org/10.3109/03639045.2011.645834.

Ashworth, C.R., Matthews, R.P., Welton, T., Hunt, P.A., 2016. Doubly ionic hydrogen bond interactions within the choline chloride-urea deep eutectic solvent †. Phys. Chem. Chem. Phys. 18, 18145. https://doi.org/10.1039/c6cp02815b.

Benvenutti, L., Zielinski, A.A.F., Ferreira, S.R.S., 2019. Which is the best food emerging solvent: IL, DES or NADES? Trends Food Sci. Technol. 90, 133–146. https://doi.org/10.1016/J.TIFS.2019.06.003.

Chakraborty, S., Chormale, J.H., Bansal, A.K., 2021. Deep eutectic systems: An overview of fundamental aspects, current understanding and drug delivery applications. Int. J. Pharm. 610, 121203 https://doi.org/10.1016/J.IJPHARM.2021.121203.

Dai, Y., van Spronsen, J., Witkamp, G.J., Verpoorte, R., Choi, Y.H., 2013. Natural deep eutectic solvents as new potential media for green technology. Anal. Chim. Acta 766, 61–68. https://doi.org/10.1016/J.ACA.2012.12.019.

DeGoey, D.A., Cox, P.B., 2021. Drug discovery beyond the rule of five. Burger's Med. Chem. Drug Discov. 1–35 https://doi.org/10.1002/0471266949.BMC258.

Deiters, U.K., 2012. The isothermal van't Hoff equation for phase equilibria—A forgotten relation? Fluid Phase Equilib. 336, 22–27. https://doi.org/10.1016/J.FLUID.2012.08.028.

Dwamena, A.K., 2019. Recent Advances in Hydrophobic Deep Eutectic Solvents for Extraction. Separations 6 (1), 9. https://doi.org/10.3390/SEPARATIONS6010009.

Emami Riedmaier, A., Lindley, D.J., Hall, J.A., Castleberry, S., Slade, R.T., Stuart, P., Carr, R.A., Borchardt, T.B., Bow, D.A.J., Nijsen, M., 2018. Mechanistic physiologically based pharmacokinetic modeling of the dissolution and food effect of a biopharmaceutics classification system IV compound—The venetoclax story. J. Pharm. Sci. 107 (1), 495–502. https://doi.org/10.1016/J.XPHS.2017.09.027.

Faggian, M., Sut, S., Perissutti, B., Baldan, V., Grabnar, I., Dall'Acqua, S., 2016. Natural deep eutectic solvents (NADES) as a tool for bioavailability improvement: pharmacokinetics of rutin dissolved in proline/glycine after oral administration in rats: possible application in nutraceuticals. Molecules 21 (11), 1531. https://doi.org/10.3390/molecules21111531.

Feeney, O.M., Crum, M.F., McEvoy, C.L., Trevaskis, N.L., Williams, H.D., Pouton, C.W., Charman, W.N., Bergström, C.A.S., Porter, C.J.H., 2016. 50 years of oral lipid-based formulations: Provenance, progress and future perspectives. Adv. Drug Deliv. Rev. 101, 167–194. https://doi.org/10.1016/J.ADDR.2016.04.007.

Florindo, C., Romero, L., Rintoul, I., Branco, L.C., Marrucho, I.M., 2018. From phase change materials to green solvents: Hydrophobic low viscous fatty acid-based deep eutectic solvents. ACS Sustain. Chem. Eng. 6 (3), 3888–3895. https://doi.org/10.1021/ACSSUSCHEMENG.7B04235.

Fourmentin, S., Costa Gomes, M., & Lichtfouse, E. (2021). *Deep eutectic solvents for medicine, gas solubilization and extraction of natural substances*. 312.

Fredenslund, A., Jones, R.L., Prausnitz, J.M., 1975. Group-contribution estimation of activity coefficients in nonideal liquid mixtures. AIChE J. 21 (6), 1086–1099. https://doi.org/10.1002/AIC.690210607.

Ghaedi, H., Ayoub, M., Sufian, S., Hailegiorgis, S.M., Murshid, G., Khan, S.N., 2018. Thermal stability analysis, experimental conductivity and pH of phosphonium-based deep eutectic solvents and their prediction by a new empirical equation. J. Chem. Thermodyn. 116, 50–60. https://doi.org/10.1016/J.JCT.2017.08.029.

Hansen, B.B., Spittle, S., Chen, B., Poe, D., Zhang, Y., Klein, J.M., Horton, A., Adhikari, L., Zelovich, T., Doherty, B.W., Gurkan, B., Maginn, E.J., Ragauskas, A., Dadmun, M., Zawodzinski, T.A., Baker, G.A., Tuckerman, M.E., Savinell, R.F., Sangoro, J.R., 2021. Deep eutectic solvents: A review of fundamentals and applications. Chem. Rev. 121 (3), 1232–1285. https://doi.org/10.1021/acs.chemrev.0c00385.

Hartung, I.V., Huck, B.R., Crespo, A., 2023. Rules were made to be broken. Nature Reviews Chemistry 7 (1), 3–4. https://doi.org/10.1038/s41570-022-00451-0.

Hawley, G. G. (Gessner G., & Lewis, R. J. (2002). *Hawley's condensed chemical dictionary*. 1223.

Huber, V., Hioe, J., Touraud, D., Kunz, W., 2022. Uncovering the curcumin solubilization ability of selected natural deep eutectic solvents based on quaternary ammonium compounds. J. Mol. Liq. 361, 119661 https://doi.org/10.1016/J.MOLLIQ.2022.119661.

Jakalian, A., Jack, D.B., Bayly, C.I., 2002. Fast, efficient generation of high-quality atomic charges. AM1-BCC model: II. Parameterization and validation. J. Comput. Chem. 23 (16), 1623–1641. https://doi.org/10.1002/JCC.10128.

Jeliński, T., Przybyłek, M., Cysewski, P., 2019. Natural deep eutectic solvents as agents for improving solubility. Stability Deliv. Curcumin. https://doi.org/10.1007/s11095-019-2643-2.

Jiesheng, L., Yuanyuan, Y., Xiang, H., 2016. Research on the preparation and properties of lauric acid/expanded perlite phase change materials. Energ. Build. 110, 108–111. https://doi.org/10.1016/J.ENBUILD.2015.10.043.

Koehl, N.J., Holm, R., Kuentz, M., Griffin, B.T., 2019. New insights into using lipid based suspensions for "Brick Dust" Molecules: Case study of nilotinib. Pharma. Res. 36 (4) https://doi.org/10.1007/S11095-019-2590-Y.

Koehl, N.J., Henze, L.J., Bennett-Lenane, H., Faisal, W., Price, D.J., Holm, R., Kuentz, M., Griffin, B.T., 2021. In silico, in vitro, and in vivo evaluation of precipitation inhibitors in supersaturated lipid-based formulations of venetoclax. Mol. Pharm. 18 (6), 2174–2188. https://doi.org/10.1021/ACS.MOLPHARMACEUT.0C00645/ASSET/IMAGES/LARGE/MP0C00645_0006.JPEG.

Koehl, N.J., Henze, L.J., Holm, R., Kuentz, M., Keating, J.J., De Vijlder, T., Marx, A., Griffin, B.T., 2022. Lipophilic salts and lipid-based formulations for bridging the food effect gap of venetoclax. J. Pharm. Sci. 111 (1), 164–174. https://doi.org/10.1016/J.XPHS.2021.09.008.

Krieger, E., Vriend, G., 2014. YASARA View - molecular graphics for all devices - from smartphones to workstations. Bioinformatics (Oxford, England) 30 (20), 2981–2982. https://doi.org/10.1093/BIOINFORMATICS/BTU426.

Kuentz, M., 2019. Drug supersaturation during formulation digestion, including real-time analytical approaches. Adv. Drug Deliv. Rev. 142, 50–61. https://doi.org/10.1016/J.ADDR.2018.11.003.

Li, Z., Lee, P.I., 2016. Investigation on drug solubility enhancement using deep eutectic solvents and their derivatives. Int. J. Pharm. 505 (1–2), 283–288. https://doi.org/10.1016/J.IJPHARM.2016.04.018.

Liu, Y., Friesen, J.B., McAlpine, J.B., Lankin, D.C., Chen, S.-N., Pauli, G.F., 2018. Natural deep eutectic solvents: Properties, applications, and perspectives. J. Nat. Prod. 81 (3), 679–690. https://doi.org/10.1021/acs.jnatprod.7b00945.

Marques, M., 2004. Dissolution media simulating fasted and fed states. Dissolut. Technol. 11 (2), 16. https://doi.org/10.14227/DT110204P16.

Martins, M.A.R., Pinho, S.P., Coutinho, J.A.P., 2019. Insights into the nature of eutectic and deep eutectic mixtures. J. Solution Chem. 48 (7), 962–982. https://doi.org/10.1007/s10953-018-0793-1.

Moreno, E., Cordobilla, R., Calvet, T., Cuevas-Diarte, M.A., Gbabode, G., Negrier, P., Mondieig, D., Oonk, H.A.J., 2007. Polymorphism of even saturated carboxylic acids from n-decanoic to n-eicosanoic acid. New J. Chem. 31 (6), 947–957. https://doi.org/10.1039/B700551B.

Morrison, H.G., Sun, C.C., Neervannan, S., 2009. Characterization of thermal behavior of deep eutectic solvents and their potential as drug solubilization vehicles. Int. J. Pharm. 378 (1–2), 136–139. https://doi.org/10.1016/J.IJPHARM.2009.05.039.

Oyoun, F., Toncheva, A., Henríquez, L.C., Grougnet, R., Laoutid, F., Mignet, N., Alhareth, K., Corvis, Y., 2023. Deep eutectic solvents: An eco-friendly design for drug engineering. ChemSusChem 16 (20), e202300669. https://doi.org/10.1002/CSSC.202300669.

Palmelund, H., Andersson, M.P., Asgreen, C.J., Boyd, B.J., Rantanen, J., Löbmann, K., 2019. Tailor-made solvents for pharmaceutical use? Experimental and computational approach for determining solubility in deep eutectic solvents (DES). Int. J. Pharma.: X 1, 100034. https://doi.org/10.1016/J.IJPX.2019.100034.

Palmelund, H., Boyd, B.J., Rantanen, J., Löbmann, K., 2020. Influence of water of crystallization on the ternary phase behavior of a drug and deep eutectic solvent. J. Mol. Liq. 315, 113727 https://doi.org/10.1016/J.MOLLIQ.2020.113727.

Palmelund, H., Eriksen, J.B., Bauer-Brandl, A., Rantanen, J., Löbmann, K., 2021. Enabling formulations of aprepitant: in vitro and in vivo comparison of nanocrystalline, amorphous and deep eutectic solvent based formulations. Int. J. Pharma.: X 3, 100083. https://doi.org/10.1016/J.IJPX.2021.100083.

Palmelund, H., Rantanen, J., Löbmann, K., 2021. Deliquescence behavior of deep eutectic solvents. Appl. Sci. 11, 1601. https://doi.org/10.3390/app11041601.

Panbachi, S., Beranek, J., Kuentz, M., 2023. Polymer-embedded deep eutectic solvents (PEDES) as a novel bio-enabling formulation approach. Eur. J. Pharm. Sci. 186, 106463 https://doi.org/10.1016/J.EJPS.2023.106463.

Porter, C.J.H., Pouton, C.W., Cuine, J.F., Charman, W.N., 2008. Enhancing intestinal drug solubilisation using lipid-based delivery systems. Adv. Drug Deliv. Rev. 60 (6), 673–691. https://doi.org/10.1016/J.ADDR.2007.10.014.

Pouton, C.W., 2006. Formulation of poorly water-soluble drugs for oral administration: Physicochemical and physiological issues and the lipid formulation classification system. Eur. J. Pharm. Sci. 29 (3–4), 278–287. https://doi.org/10.1016/J.EJPS.2006.04.016.

Prathapa, S.J., Slabbert, C., Fernandes, M.A., Lemmerer, A., 2018. Structure determination of fatty acid ester biofuels via in situ cryocrystallisation and single crystal X-ray diffraction. CrstEngComm 21 (1), 41–52. https://doi.org/10.1039/C8CE01673A.

Prigogine, I., & Defay, R. (1954). Chemical Thermodynamics: Treatise on Thermodynamics Based on Methods of Gibbs and De Donder. In D. H. Everett (Ed.), *Chemical Thermodynamics: Vol. I*. Longmans Green & Co Ltd. https://archive.org/details/chemicalthermody0000ipri.

Ramón, D. J., & Guillena, G. (2019). Deep eutectic solvents: Synthesis, properties, and applications. *Deep Eutectic Solvents: Synthesis, Properties, and Applications*, 1–370. https://doi.org/10.1002/9783527818488.

Rowe, R., Sheskey, P., & Quinn, M. E. (1994). *Handbook of Pharmaceutical Excipients*.

Shah, V.P., Amidon, G.L., 2014. GL Amidon, H. Lennernas, VP Shah, and JR Crison. A theoretical basis for a biopharmaceutic drug classification: The correlation of in vitro drug product dissolution and in vivo bioavailability, Pharm Res 12, 413–420, 1995—Backstory of BCS. The AAPS journal 16, 894–898. https://doi.org/10.1208/S12248-014-9620-9/METRICS.

Skjold-Jorgensen, S., Kolbe, B., Gmehling, J., Rasmussen, P., 1979. Vapor-liquid equilibria by UNIFAC group contribution. Revision and extension. Industrial & Engineering Chemistry Process Design and Development 18 (4), 714–722. https://doi.org/10.1021/i260072a024.

Sut, S., Faggian, M., Baldan, V., Poloniato, G., Castagliuolo, I., Grabnar, I., Perissutti, B., Brun, P., Maggi, F., Voinovich, D., Peron, G., 2017. Natural Deep Eutectic Solvents (NADES) to enhance berberine absorption: An in vivo pharmacokinetic study. Molecules 22 (11), 1921. https://doi.org/10.3390/molecules22111921.

Tolmachev, D., Lukasheva, N., Ramazanov, R., Nazarychev, V., Borzdun, N., Volgin, I., Andreeva, M., Glova, A., Melnikova, S., Dobrovskiy, A., Silber, S.A., 2022. Computer simulations of deep eutectic solvents: Challenges, solutions, and perspectives. International journal of molecular sciences 23 (2), 645. https://doi.org/10.3390/IJMS23020645.

Umerska, A., Bialek, K., Zotova, J., Skotnicki, M., Tajber, L., 2020. Anticrystal engineering of ketoprofen and ester local anesthetics: Ionic liquids or deep eutectic mixtures? Pharmaceutics 12 (4). https://doi.org/10.3390/PHARMACEUTICS12040368.

Van Osch, D.J.G.P., Dietz, C.H.J.T., Warrag, S.E.E., Kroon, M.C., 2020. The curious case of hydrophobic deep eutectic solvents: A story on the discovery, design, and applications. ACS Sustain. Chem. Eng. 8 (29), 10591–10612. https://doi.org/10.1021/ACSSUSCHEMENG.0C00559/ASSET/IMAGES/MEDIUM/SC0C00559_0005.GIF.

Wang, L., Meng, D., 2010. Fatty acid eutectic/polymethyl methacrylate composite as form-stable phase change material for thermal energy storage. Appl. Energy 87 (8), 2660–2665. https://doi.org/10.1016/J.APENERGY.2010.01.010.

Wang, J., Wolf, R.M., Caldwell, J.W., Kollman, P.A., Case, D.A., 2004. Development and testing of a general amber force field. J. Comput. Chem. 25 (9), 1157–1174. https://doi.org/10.1002/JCC.20035.

Wolbert, F., Brandenbusch, C., Sadowski, G., 2019. Selecting excipients forming therapeutic deep eutectic systems-A mechanistic approach. Mol. Pharm. 16 https://doi.org/10.1021/acs.molpharmaceut.9b00336.

Zainal-Abidin, M.H., Hayyan, M., Wong, W.F., 2021. Hydrophobic deep eutectic solvents: Current progress and future directions. J. Ind. Eng. Chem. 97, 142–162. https://doi.org/10.1016/J.JIEC.2021.03.011.

Zhou, K., Liu, B., 2022. Control techniques of molecular dynamics simulation. Mol. Dyn. Simul. 67–96 https://doi.org/10.1016/B978-0-12-816419-8.00008-8.